Targeting proapoptotic protein BAD inhibits survival and self-renewal of cancer stem cells

KSR Sastry*[,1], MA Al-Muftah[2], Pu Li[3], MK Al-Kowari[2], E Wang[4], A Ismail Chouchane[4], D Kizhakayil[1], G Kulik[5,6], FM Marincola[7], A Haoudi[2] and L Chouchane*[,1]

Emerging evidence suggests that the resistance of cancer stem cells (CSC) to many conventional therapies is one of the major limiting factors of cancer therapy efficacy. Identification of mechanisms responsible for survival and self-renewal of CSC will help design new therapeutic strategies that target and eliminate both differentiated cancer cells and CSC. Here we demonstrated the potential role of proapoptotic protein BAD in the biology of CSC in melanoma, prostate and breast cancers. We enriched $CD44^+/CD24^-$ cells (CSC) by tumorosphere formation and purified this population by FACS. Both spheres and CSC exhibited increased potential for proliferation, migration, invasion, sphere formation, anchorage-independent growth, as well as upregulation of several stem cell-associated markers. We showed that the phosphorylation of BAD is essential for the survival of CSC. Conversely, ectopic expression of a phosphorylation-deficient mutant BAD induced apoptosis in CSC. This effect was enhanced by treatment with a BH3-mimetic, ABT-737. Both pharmacological agents that inhibit survival kinases and growth factors that are involved in drug resistance delivered their respective cytotoxic and protective effects by modulating the BAD phosphorylation in CSC. Furthermore, the frequency and self-renewal capacity of CSC was significantly reduced by knocking down the BAD expression. Consistent with our *in vitro* results, significant phosphorylation of BAD was found in $CD44^+$ CSC of 83% breast tumor specimens. In addition, we also identified a positive correlation between BAD expression and disease stage in prostate cancer, suggesting a role of BAD in tumor advancement. Our studies unveil the role of BAD in the survival and self-renewal of CSC and propose BAD not only as an attractive target for cancer therapy but also as a marker of tumor progression.
Cell Death and Differentiation (2014) **21,** 1936–1949; doi:10.1038/cdd.2014.140; published online 12 September 2014

Although tumors initially respond positively to anti-cancer agents, several cancers, despite the best care and significant improvements in treatment, recur and progress to advanced stages of the disease. The mechanisms underlying this recurrence and metastasis are not clearly understood. Over the past decade, substantial evidence supported the cancer stem cell (CSC) hypothesis as a viable explanation for the initiation, progression and recurrence of cancer. According to this hypothesis, each tumor harbors a small subpopulation of specialized cells among cellular heterogeneity, known as CSC. These cells exhibit self-renewal property that drives tumorigenesis and plasticity to differentiate into multiple cell types contributing to tumor cellular heterogeneity. Support for this hypothesis came from the studies by Lapidot *et al.* who identified tumor-initiating cells in acute myeloid leukemia.[1,2] Subsequently, CSCs have been identified in several cancers.[3–10]

Accumulating evidence suggests that current cancer therapies can only shrink tumors as they target and kill the differentiated cancer (DC) cells, but are unable to target the rare CSC population.[11,12] Thus, despite a wealth of information on DC cells, the active survival and self-renewal pathways in CSCs have not been characterized thoroughly. An understanding of the molecular mechanisms involved in the survival, self-renewal and resistance of CSCs to current therapeutic regimens is of immense clinical interest. This information will help in developing novel strategies for more effective treatments for cancer.

Most anti-cancer drugs exert their effects through triggering the apoptotic pathways. However, malignant cancer cells can escape apoptosis by altering the expression level of proapoptotic and antiapoptotic BCL-2 family members. Considering the potential role of BCL-2 family members in tumorigenesis and cancer cell survival, their role in CSC
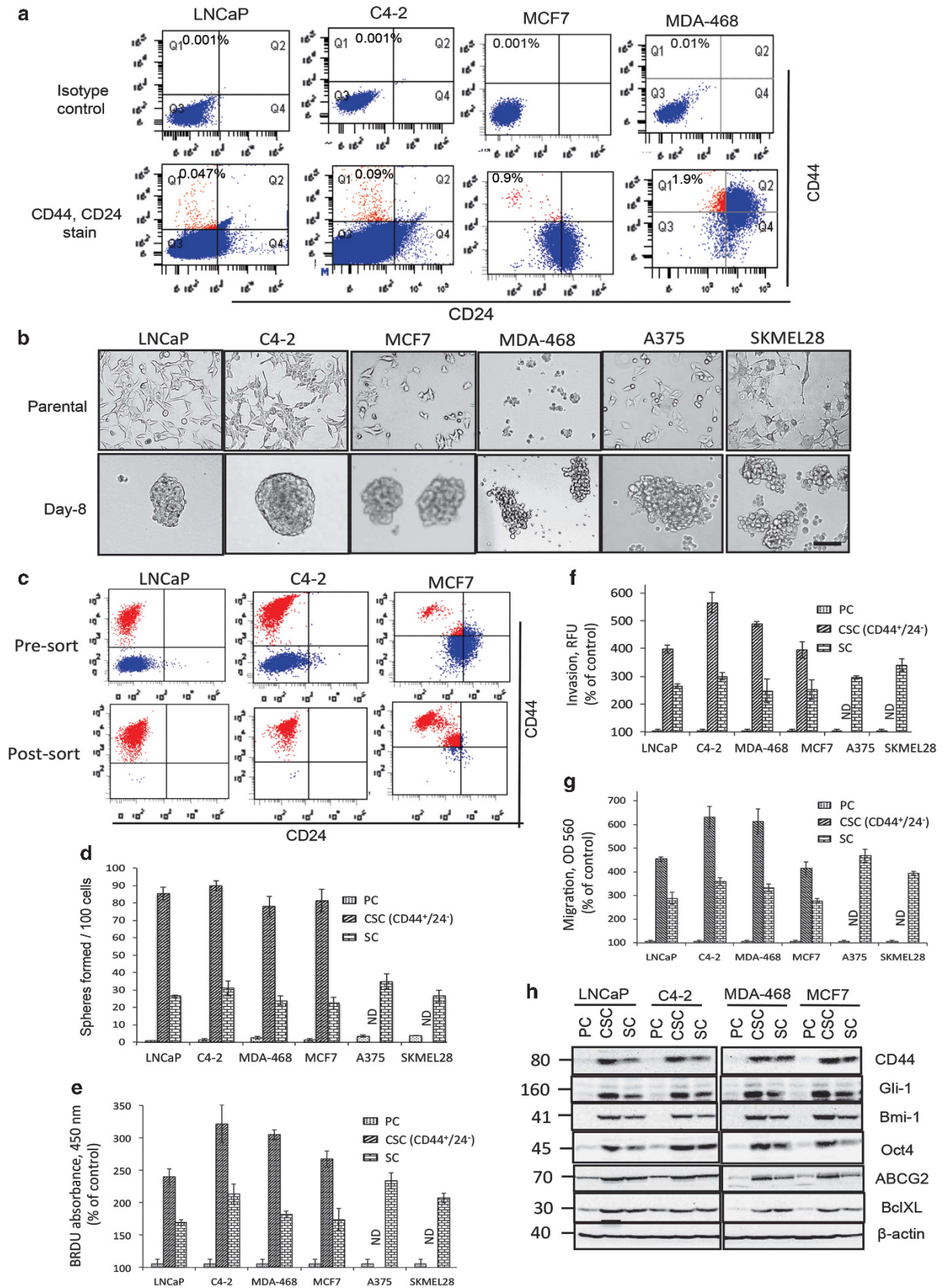
Figure 1 For caption see next page.

biology has been increasingly studied.[13,14] BAD (BCL2-antagonist of cell death) is a member of the BH3-only BCL-2 family protein that when dephosphorylated promotes apoptosis by heterodimerizing with the antiapoptotic proteins BCL-XL and BCL-2.[15] The cytotoxic effects of BAD are controlled by mechanisms that regulate its phosphorylation on at least two distinct serine residues, S112 and S136.[16–18] Previously, we showed that phosphorylation at either site is sufficient to protect prostate cancer cells from apoptosis.[19–21] We also showed that BAD promotes prostate tumor growth in mouse models.[22] Clinically, while BAD expression was associated with relapse in tamoxifen-treated breast cancer patients,[23,24] phospho-BAD expression was associated with cisplatin resistance and poor overall survival in ovarian cancer.[25]

Our previous findings along with other reports showing the role of BAD in the apoptosis modulation and growth of DC cells[19,22,26] prompted us to explore the potential role of BAD in the biology of CSCs. We started our investigation by assessing the role of BAD in survival and self-renewal of CSCs. As we observed a significant role for BAD in CSC's biology, we extended our work to assess the BAD phosphorylation in CSCs of breast cancer patient tumors and for a potential correlation between BAD expression and disease progression in prostate cancer.

Results

Identification, enrichment, purification and characterization of CSCs.
We first attempted to identify and assess the percentage of CSCs in the cancer cell lines of prostate, breast and melanoma. Flow cytometry analysis of cancer cells stained with antibodies that recognize widely used stem cell-associated markers CD44 and CD24 revealed varying abundance of $CD44^{+/high}CD24^{-/low}$ CSC population. Although LNCaP and C4-2 exhibited 0.04 and 0.09%, respectively, MCF7 and MDA-468 displayed more prevalent population of about 1–2% (Figure 1a).

As the CSC-specific markers are not perfect and not well defined for melanoma,[27,28] the sphere-formation method remains the standard method to detect and enrich CSCs.[5–9] As shown in Figure 1b, all cell lines generated tumorospheres, and flow cytometry analyses showed that $CD44^+$ $CD24^-$ population was highly enriched in tumorospheres (Supplementary Figure S1A). We sorted $CD44^+CD24^-$ cells from spheres of prostate and breast cancer using fluorescence-activated cell sorting (FACS) and achieved a purity of >95% as judged by postsorting flow analysis (Figure 1c).

Compared with parental cells (PC), the stem cell-associated properties of both purified $CD44^+CD24^-$ cells and spheres exhibited significantly increased proliferation potential, migration, invasion, anchorage-independent growth on soft agar (clonogenicity) and sphere-forming capacity (Figures 1d–g, Supplementary Figure S1B, Supplementary Table S1). The $CD44^+CD24^-$ cells purified directly from PC and from tumorospheres displayed similar stem cell-associated characteristics (Supplementary Figures S1C–E). In addition, compared with PC, sorted $CD44^+CD24^-$ cells and tumorospheres expressed increased quantities of CD44 stem cell marker, several transcription factors that are essential for self-renewal of stem cells, antiapoptotic protein BCL-XL and multidrug transporter ABCG2 (Figure 1h). Similarly, melanoma spheres exhibited increased expression of stem cell-associated markers (Supplementary Figure S1F). Indeed, such $CD44^+CD24^-$ cells from prostate and breast cancer cells exhibited increased tumor-initiating capacity compared with their PC in severe combined immunodeficiency mice.[29–33] The sorted $CD44^+CD24^-$ cells are hereafter referred to as CSCs. Collectively, our data suggest that both CSCs and spheres exhibited diverse stem cell-associated characteristics, consistent with previous reports.[5–9]

CSCs overexpressed BAD with elevated phosphorylation.
As CSCs are resistant to drugs[11] and phosphorylated BAD correlates with drug resistance in cancer patients,[25] we determined the level of BAD expression and phosphorylation in CSCs and tumorospheres. CSCs and spheres of LNCaP, C4-2, MDA-468 and MCF7 exhibited substantially elevated levels of BAD compared with their PC. Similarly, while tumorospheres of A375 exhibited increased BAD expression, the spheres of SKMEL28 maintained BAD expression similar to their PC (Figure 2a, Supplementary Figure S2A). The CSCs purified directly from PC and from tumorospheres exhibited similar level of increased BAD expression compared with PC (Supplementary Figure S2B). Although BAD is kept phosphorylated at both S112 and S136 in CSCs and spheres of breast and prostate cancer, S112 phosphorylation was predominant in melanoma spheres (Figure 2b, Supplementary Figure S2C). The phosphorylation of BAD at S155 was not consistently elevated (not shown). To corroborate our in vitro observation, we assessed BAD phosphorylation in biopsies of breast cancer patient tumors. Significant phosphorylation of BAD was found in $CD44^+$ CSC of 83% (34 of 41) breast tumors (Figure 2c). The latter result demonstrates that BAD phosphorylation is not only

Figure 1 Identification, enrichment, purification and characterization of CSCs. (**a**) Single-cell suspensions of the indicated cells were stained with isotype control or CD44 and CD24 antibodies and analyzed by flow cytometry. Upper left quadrant (Q1) represents CSC ($CD44^{+/high}CD24^{-/low}$) population as shown in red dots. The percentage of CSCs is indicated in Q1. (**b**) Tumorosphere formation: Cancer cells were grown in normal 10% FBS medium (parental) or sphere medium for the indicated time. Phase-contrast images are shown. Formation of unattached spheres can be observed. Scale bar = 100 μm. (**c**) Double stained cells were FAC-sorted and reanalyzed (postsorting) immediately after the sorting. (**d**) Parental, sorted CSCs and sphere-derived cells at 1 cell/well in 96-well plate were placed, and sphere-forming efficiency was compared. The number of spheres (>100 μm) formed was counted under microscope. (**e**) Extended proliferative capacity of CSCs and spheres compared with parental cells: In all, 10^4 indicated cells were seeded in 96-well plate and, 3 days after, cells were incubated with 10 μM BrdU, followed by anti-BrdU antibody-HRP. (**f**) Increased invasion capacity of CSCs and spheres: Indicated cells were seeded and allowed to invade toward the bottom side of the membrane containing growth factor supplements for 24 h. Fluorescence measurements were taken according to assay instructions. (**g**) Increased migration capacity of CSCs and spheres: Indicated cells were seeded and allowed to migrate towards growth factor supplements for 24 h. Colorimetric measurements were taken according to assay instructions. (**h**) Upregulation of stemness markers in CSCs and spheres as compared with parental cells was confirmed by western blotting using the indicated antibodies. The error bars represent S.D. of the biological triplicates. All experiments presented in this figure are representative of at least three independent experiments
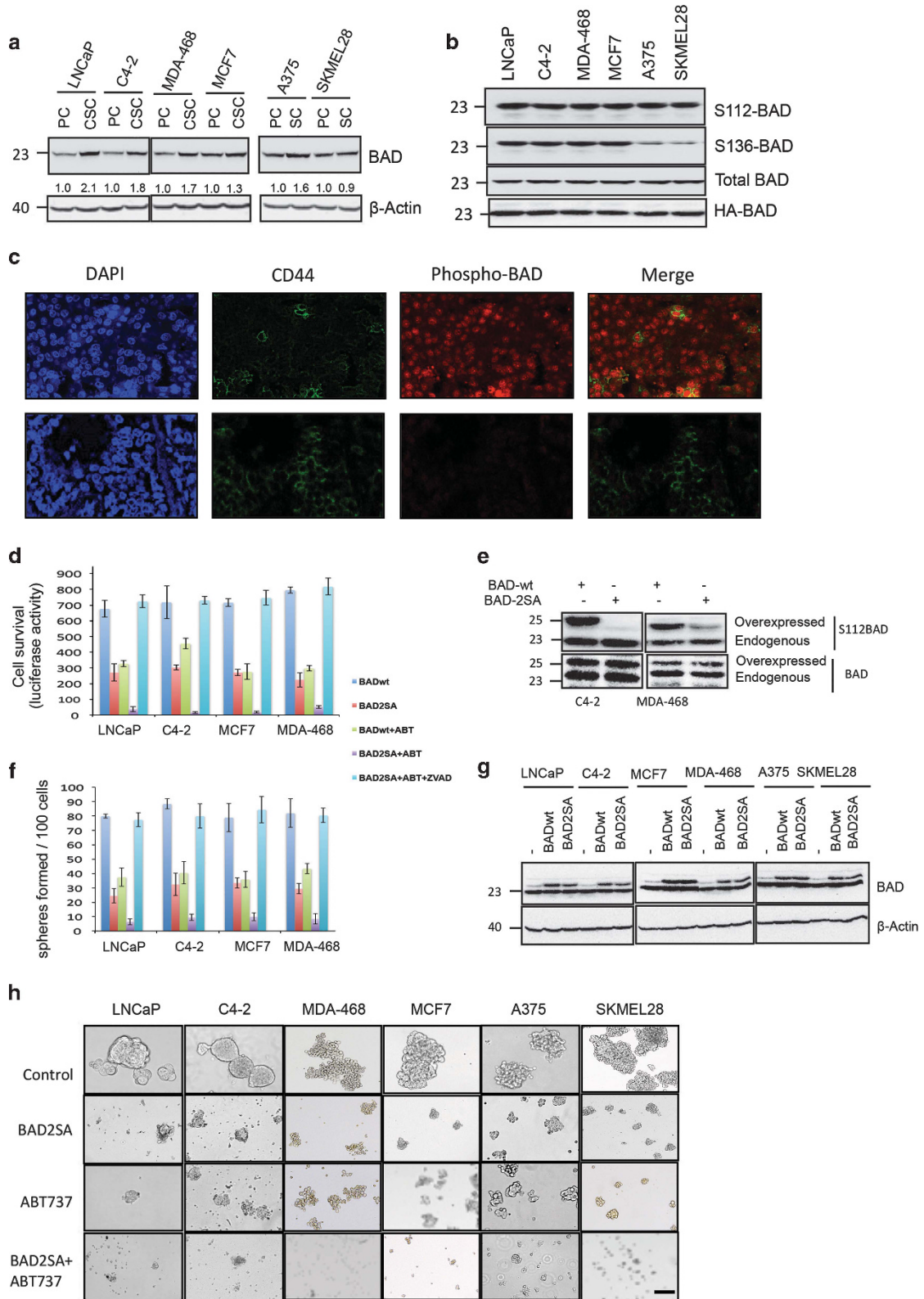
Figure 2 For caption see next page.

limited to CSCs obtained from *in vitro* cell culture model but also occurred in patient tumors. These results suggest that CSCs express higher levels of BAD with elevated phosphorylation, suggesting dependence of CSCs on this protein.

BAD phosphorylation is prerequisite for CSC survival.
To determine the role of BAD phosphorylation in CSC survival, we co-infected CSCs with lentiviral vectors that encode luciferase and either wild-type BAD (BADwt) or a mutant BAD (BAD2SA) in which both S112 and S136 sites were mutated to alanine and thus no longer be phosphorylated. The cell viability was judged by measuring the luciferase activity in the cell lysates as described.[19,34] The survival of BAD2SA-expressing CSCs was substantially decreased compared with BADwt-CSCs (Figure 2d). As CSCs expressed elevated levels of antiapoptotic BCL-XL as shown in Figure 1h, and endogenous BAD was still phosphorylated in BAD2SA-CSCs (Figure 2e), we tested whether BH3-mimetic can further sensitize CSCs to BAD2SA-mediated cell death. ABT-737, a BH3-mimetic that can inhibit the function of Bcl2 and BclXL,[35] promoted a strong synergistic apoptotic effect that further decreased the survival of BAD2SA-expressing CSCs. Prior treatment of BAD2SA-expressing CSCs with a pan-caspase inhibitor ZVAD-FMK completely rescued them from apoptosis, further supporting the proapoptotic effects of BAD2SA on CSCs. To confirm these data, single-cell suspensions of the CSCs expressing BADwt or BAD2SA were used in sphere-forming assay and found that the quantity of spheres with BAD2SA alone or in combination with ABT-737 was highly reduced compared with BADwt-expressing CSCs (Figure 2f). Figure 2g shows the expression level of BADwt and BAD2SA. Similar effects of BAD2SA were observed with tumorospheres. BAD2SA induced robust apoptosis that resulted in the disintegration of spheres (Figure 2h and Supplementary Figures S2D and E). Together, our data suggest that BAD phosphorylation is critical for the survival of CSCs.

Active survival kinases in CSCs deliver their effects through BAD. Substantial number of cancers exhibits increased PI3K/Akt, mitogen-activated protein kinase (MAPK) and Raf signaling.[36–38] Although these pathways were shown to modulate survival and self-renewal of

CSCs, the precise downstream molecules controlling these properties have not been thoroughly investigated.[39] To test whether Akt-induced survival effects might be mediated through BAD, we inhibited Akt in CSCs and tumorospheres of prostate with LY294002, a PI3K inhibitor, and assessed apoptosis and BAD phosphorylation. Apoptosis was quantified by measuring the caspase activity and confirmed by measuring the cleaved PARP and cleaved caspase-3 in the cell lysates. Treatment of prostatospheres and CSCs with LY294002 resulted in apoptosis and dephosphorylation of BAD at S112 and S136 (Figures 3a–c; Supplementary Figures S3A and B), suggesting a correlation between these two events. To confirm these results, we performed sphere-forming assay using single-cell suspensions obtained from LY294002-treated or control spheres. There was a significant decline in secondary sphere number in LY294002-treated cultures compared with control (Figure 3d). In spheres and CSCs obtained from MDA-468, LY294002 induced dephosphorylation of BAD specifically at S136, whereas a MEK inhibitor PD98059 decreased S112 phosphorylation. Combination of LY294002 and PD98059 dephosphorylated both S112 and S136. Consistent with these observations, treatment with either of these inhibitors displayed only partial effects on cell survival, and simultaneous suppression of MAPK and PI3K/Akt substantially enhanced apoptosis (Figures 3a–d, Supplementary Figures S3A and B). Similarly, treatment of melanoma spheres with Raf inhibitor Vemurafenib, a widely used drug for the treatment of melanoma patients, induced apoptosis and reduced both S112 phosphorylation and sphere-formation capacity (Figures 3a–d).

To establish that BAD expression is essential to induce apoptosis in CSCs, we silenced BAD expression using BAD-specific small hairpin RNA (shRNA), which dramatically reduced BAD expression (Figure 3e). BAD-silenced spheres became insensitive to inhibitors compared with scr-shRNA-expressing spheres (Figure 3f). Similar results were obtained with sorted CSCs (Supplementary Figure S3C). Together, these results suggest that the key regulatory kinases such as Akt, MAPK and Raf deliver their survival effects, at least in part, by modulating BAD phosphorylation in CSCs.

Survival agonists exert their antiapoptotic effects by modulating BAD phosphorylation in CSCs. Because the biological effects driven by estrogen receptor (ER) are

Figure 2 BAD phosphorylation is essential for CSC survival. (**a**) Expression of BAD in PC, CSCs (CD44 + CD24 −) and spheres (SC) was compared using western blotting. BAD antibodies were used to detect endogenous BAD. Equal loading was judged by β-actin. The numbers under each lane are intensity of the band relative to that of parental cells. (**b**) BAD is constitutively phosphorylated in spheres: Tumorospheres were infected with lentiviral vector expressing HA-BAD. Two days after infection, spheres were placed in supplement-free basal Dulbecco's modified Eagle's medium (DMEM) medium for 3 h and lysed. HA-BAD was immunoprecipitated using 12CA5 antibodies and immunoblotted with the indicated antibodies. (**c**) Immunofluorescence analysis of CSC in breast tumors: Upper panel: 5-μm sections were stained with mouse anti-CD44 and rabbit anti-phospho-BAD antibodies, followed by anti-mouse IgG-AlexaFluor-488 (green) and anti-rabbit IgG-AlexaFluor-647 (red) secondary antibodies (Invitrogen). Nuclei were stained with 4,6-diamidino-2-phenylindole (blue). Representative confocal images are shown at $\times$40 magnification. Note that BAD phosphorylation (red) is clearly seen in CD44 stained CSC (green). Lower panel: Phospho-BAD antibodies were preincubated with the immunizing peptide and then used to stain tumor sections. Lack of phospho-BAD staining confirms the specific staining observed in upper panel. (**d**) CSCs were infected with lentiviral vectors expressing BADwt or BAD2SA and luciferase. After 24 h, CSCs were incubated in supplement-free DMEM containing 10 μM ABT-737 for 24 h, and luciferase activity was measured from cell lysates. Where indicated, 3 h after infection 20 μM of pan-caspase inhibitor Z-VAD-FMK was added to the culture and incubated until cell lysis. (**e**) Endogenous BAD is kept phosphorylated in BADwt or BAD2SA expressing CSCs: CSCs were infected with either BADwt or BAD2SA, and cell lysates were probed with the tindicated antibodies. (**f**) Sphere-forming assay was performed using cells in panel (**d**), and the number of spheres formed was counted. (**g**) Expression levels of BADwt and BAD2SA in cell lysates are shown. (**h**) BAD2SA induces apoptosis in spheres: Phase-contrast images of spheres treated as in panel (**d**) are shown. Scale bar = 100 μm. The error bars represent S.D. of the biological triplicates. All experiments presented in this figure are representative of three independent experiments
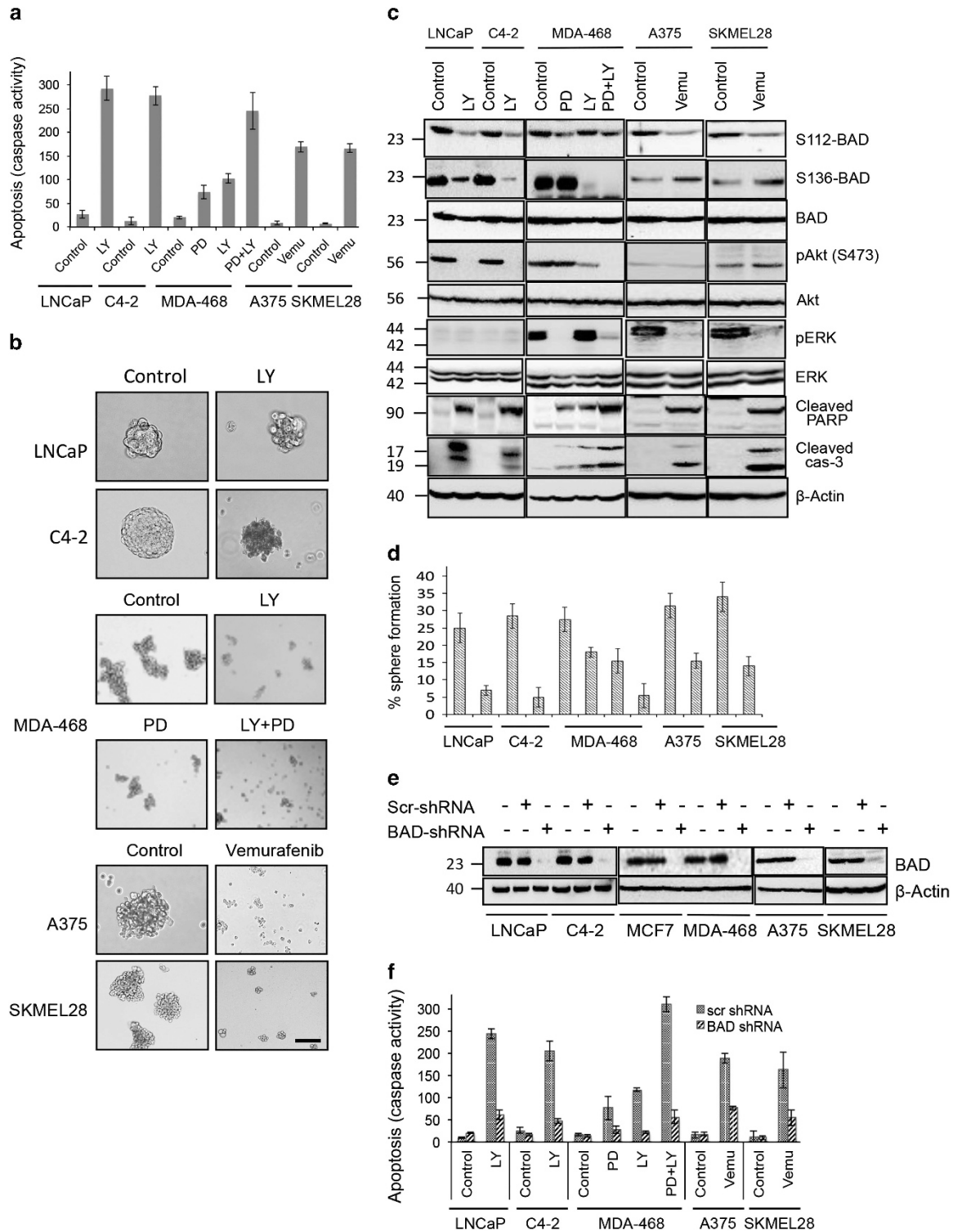
Figure 3 Drugs and pharmacological inhibitors mediate their cytotoxic effects in CSCs through BAD dephosphorylation: (**a**) Spheres derived from the indicated cell lines were starved for 12 h and treated with 20 μM LY, 50 μM PD or 20 μM Vemurafenib, and caspase activity in the cell lysates was measured using the fluorogenic substrate Ac-DEVD-AMC. (**b**) Phase-contrast images of spheres treated as in panel (**a**) are shown. Scale bar = 100 μm. (**c**) BADwt-expressing spheres were treated for 3 h with the indicated inhibitors, and cell lysates were collected. HA-BAD was immunoprecipitated, and phosphorylation of BAD was detected as in Figure 2b. S112-BAD blot was stripped and reprobed with BAD antibodies. Whole-cell lysates were used to probe phospho-Akt, phospho-ERK, cleaved PARP, cleaved caspase-3 and β-actin. (**d**) Spheres in panel (**b**) were dissociated, and sphere-forming assay was performed, and the number of reformed spheres was counted. (**e**) Spheres were infected with BAD-shRNA or scrambled-shRNA lentiviral vectors, lysates were collected after 72 h and immunoblotted with antibodies against BAD and β-actin. BAD expression was substantially suppressed by BAD-shRNA. (**f**) Spheres in panel (**e**) were treated with the indicated inhibitors, and apoptosis was measured as in panel (**a**). Spheres displayed resistance to inhibitors in the absence of BAD. The error bars represent S.D. of the biological triplicates. All experiments presented in this figure are representative of three independent experiments
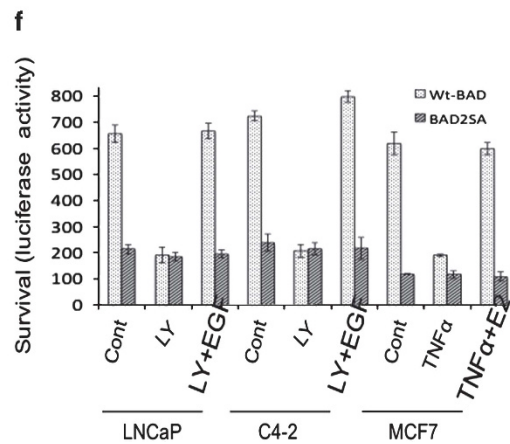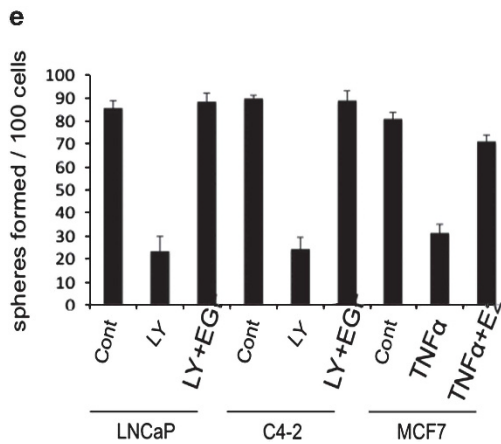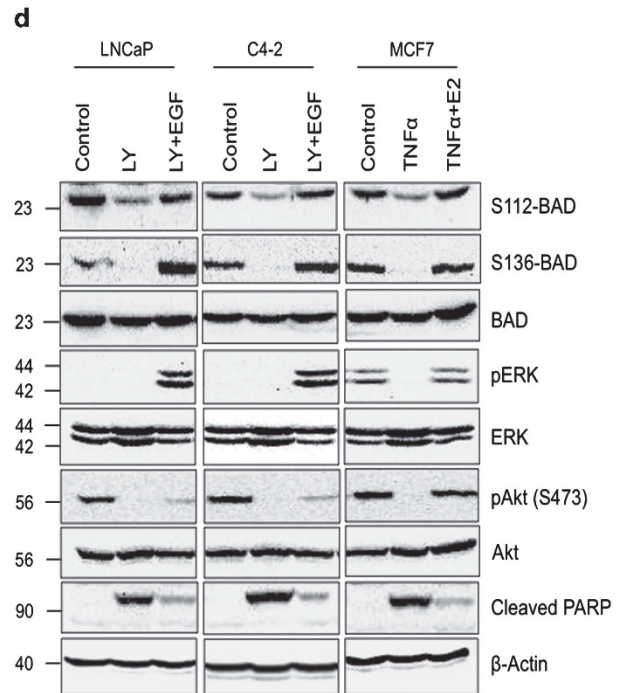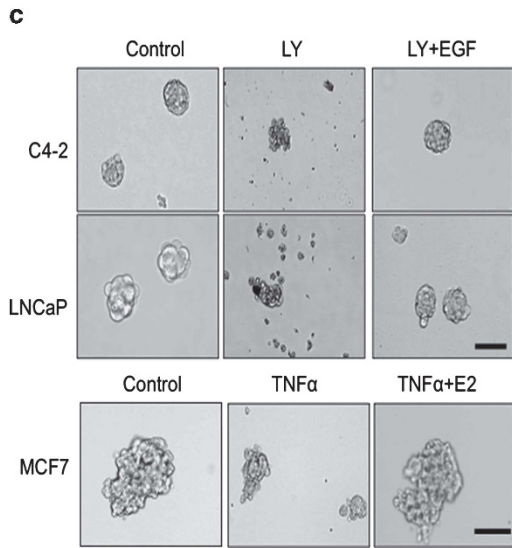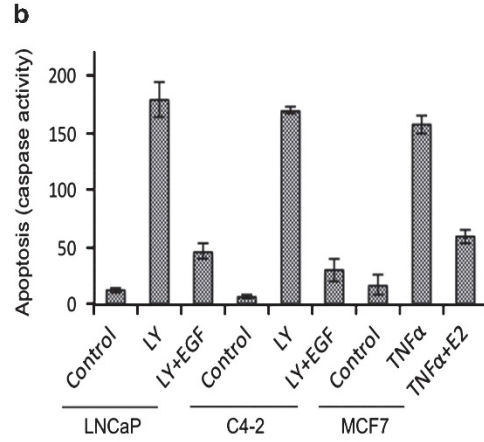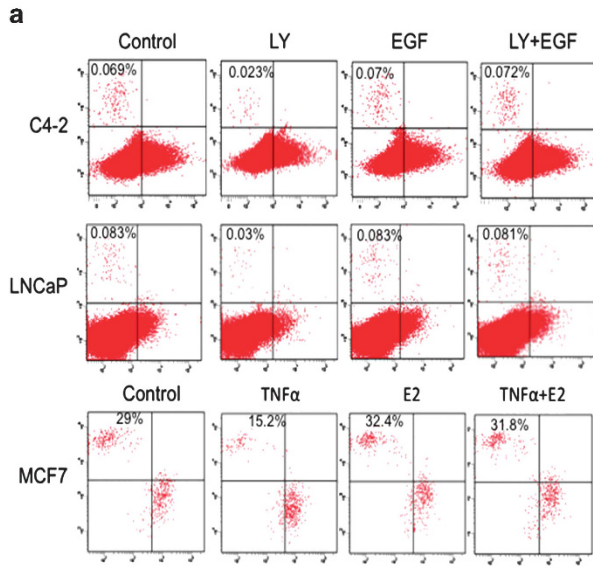
a

b

c

d

e

f

directly involved in breast cancer development and progression,[40,41] and epidermal growth factor receptor (EGFR) is overexpressed in CSCs of several tumors,[42–44] we asked whether growth factors that were known to contribute to tumorigenesis, such as EGF and 17β-estradiol (E2), mediate their antiapoptotic effects by modulating BAD phosphorylation in CSCs. Although LY294002 significantly reduced the CSC frequency in prostate cancer cells, EGF restored this frequency by protecting from LY-induced apoptosis (Figure 4a). Similarly, E2 restored the CSC fraction from tumor necrosis factor-alpha (TNFα)-induced apoptosis in MCF7 spheres. In caspase activity assays, EGF and E2 remarkably inhibited the cytotoxic effects of LY294002 and TNFα in CSCs (Figure 4b). In the presence of EGF or E2, the tumorospheres remained healthy despite the presence of LY or TNFα (Figure 4c). Both EGF and E2 restored BAD phosphorylation to a level similar to untreated cells (Figure 4d and Supplementary Figures S4A–C) and increased sphere number in sphere-forming assay, by protecting CSCs from the cytotoxicity of inhibitors (Figure 4e). To confirm this data, we ectopically expressed either BADwt or BAD2SA and assessed growth factor-induced survival. Although growth factors protected BADwt-expressing CSCs, no such protection was evident in cells that expressed BAD2SA (Figure 4f). Together, these results suggest that growth factors protect CSCs from drug-induced apoptosis by restoring BAD phosphorylation.

BAD regulates the self-renewal growth of CSCs. Given the correlation of BAD with tumor progression and metastasis, we explored whether BAD has a role in the self-renewal of CSCs. We either repressed or overexpressed BAD in cancer cells and quantified CSC population by flow cytometry. Although BAD depletion reduced CSC population by 40–50%, BAD overexpression increased CSC number about 60% compared with control cells (Figure 5a). Furthermore, BAD-silenced cells generated a strikingly lower number of spheres, with prominent decrease in their size compared with control cells (Figures 5b–d) and substantially reduced the clonogenic efficiency on soft agar (Supplementary Table S2). Compared with control spheres, the proliferation potential of BAD-knockdown cells was significantly reduced but was increased upon overexpression of BAD (Figure 5e). Similarly, the expression of several stem cell-specific markers was downregulated in BAD-knockdown cells but upregulated in BAD-overexpressed cells (Figure 5f). We obtained similar results using a different BAD-shRNA or Scr-shRNA (Supplementary Figures S5A–C). Taken together, these results clearly show that BAD has a role in modulating self-renewal of CSCs.

BAD absence delays the cell cycle progression. Next, we explored the mechanism by which BAD controls the frequency and self-renewal of CSCs. The cell death regulators of the BCL-2 family were previously shown to exert cell cycle effects.[45] To investigate whether BAD alters CSC's cell cycle progression, we cultured control or BAD-depleted cells in sphere-forming medium for 7 days. Cell cycle analysis revealed that there was 40% reduction in cells with S/G2 fraction (DNA content 2N–4N) in BAD-depleted spheres compared with control spheres (Figure 6a). We then arrested sphere cells in G0/G1 by placing them for 24 h in basal medium without growth supplements and analyzed by flow cytometry. There was more S/G2 population in control spheres compared with BADshRNA-spheres (13 vs 10%), suggesting that BAD is required for progression to S phase. Similar results were obtained with LNCaP and melanoma spheres (Figures 6a and b). Indeed, cells with S phase DNA content were actively synthesizing DNA, as revealed by 5-bromo-2'-deoxyuridine (BrdU) incorporation. Although scr-shRNA-expressing cells contained 18.7% BrdU-positive cells with DNA content 2N-4N, this number was only 8.9% in BAD-shRNA-expressing C4-2 cells. Similar trend is observed with LNCaP cells (Figure 6c). As spheres with reduced BAD expression displayed more G0/G1 cells, we tried to reveal whether any of cell cycle regulators, such as cyclin-dependent kinase 2 (cdk2) and cdk4, are responsible for this difference. Previously, cdk2 was shown to be critical for the proliferation and self-renewal of neuronal progenitor cells.[46] Thus we compared the cdk2 activity using phosphorylation-specific cdk2 antibodies. As shown in Figure 6d, cdk2 activation was substantially reduced in BAD-knockdown spheres when compared with those that expressed BAD. These data suggest that depletion of BAD is arresting CSCs in the G0/G1 phase by preventing the activation of cdk2, which resulted in the reduced frequency of CSCs in BAD-knockdown spheres.

BAD expression correlates with aggressiveness of prostate cancer. As our findings suggest that BAD modulates survival of both DCs and CSCs and promotes tumor growth in mice,[22] we tested whether BAD expression correlates with tumor aggressiveness or disease stage in prostate cancer patients. To address this, we compared BAD expression in prostate tumors ($n = 68$) and in corresponding non-malignant tumor-adjacent tissue. Quantitative real-time PCR analysis revealed that, in 46 (67.6%) cases, BAD mRNA expression was higher in the cancer tissue than in the normal tissue (Figure 7a). Our further analysis in Figure 7b shows that high-grade tumors (Gleason Score > 6) expressed significantly more BAD than low-grade tumors

Figure 4 Growth factors protect CSCs from apoptosis by inducing BAD phosphorylation. (**a**) Parental cells (LNCaP and C4-2), and sphere cells (MCF7) were treated with inhibitors and growth factors as indicated, stained with CD44 and CD24 antibodies and analyzed by flow cytometry. (**b**) Sorted CSCs were placed in supplement-free basal Dulbecco's modified Eagle's medium for 12 h and treated with 20 μM LY or 10 ng/ml TNFα. Fifteen minutes later, either 30 ng/ml EGF or 10 nM E2 was added. Caspase activity in cell lysates was measured as described in Figure 3a. (**c**) Phase-contrast images of spheres are shown. Scale bar = 100 μm. (**d**) BADwt-expressing CSCs were treated for 3 h as in panel (**a**), and cell lysates were collected. HA-BAD was immunoprecipitated, and phosphorylation of BAD was detected. S112-BAD blot was stripped and reprobed with BAD antibodies. (**e**) CSCs in panel (**b**) were used in sphere-forming assay, and the number of spheres formed was counted. (**f**) CSCs were infected with lentiviral vectors expressing BADwt or BAD2SA and luciferase. Two days later, cells were treated with the indicated inhibitors and growth factors, and luciferase activity was measured from cell lysates. BAD2SA-expressing CSCs were not protected from growth factors. The error bars represent S.D. of the biological triplicates. All experiments presented in this figure are representative of three independent experiments

a

b

c

d

e

f
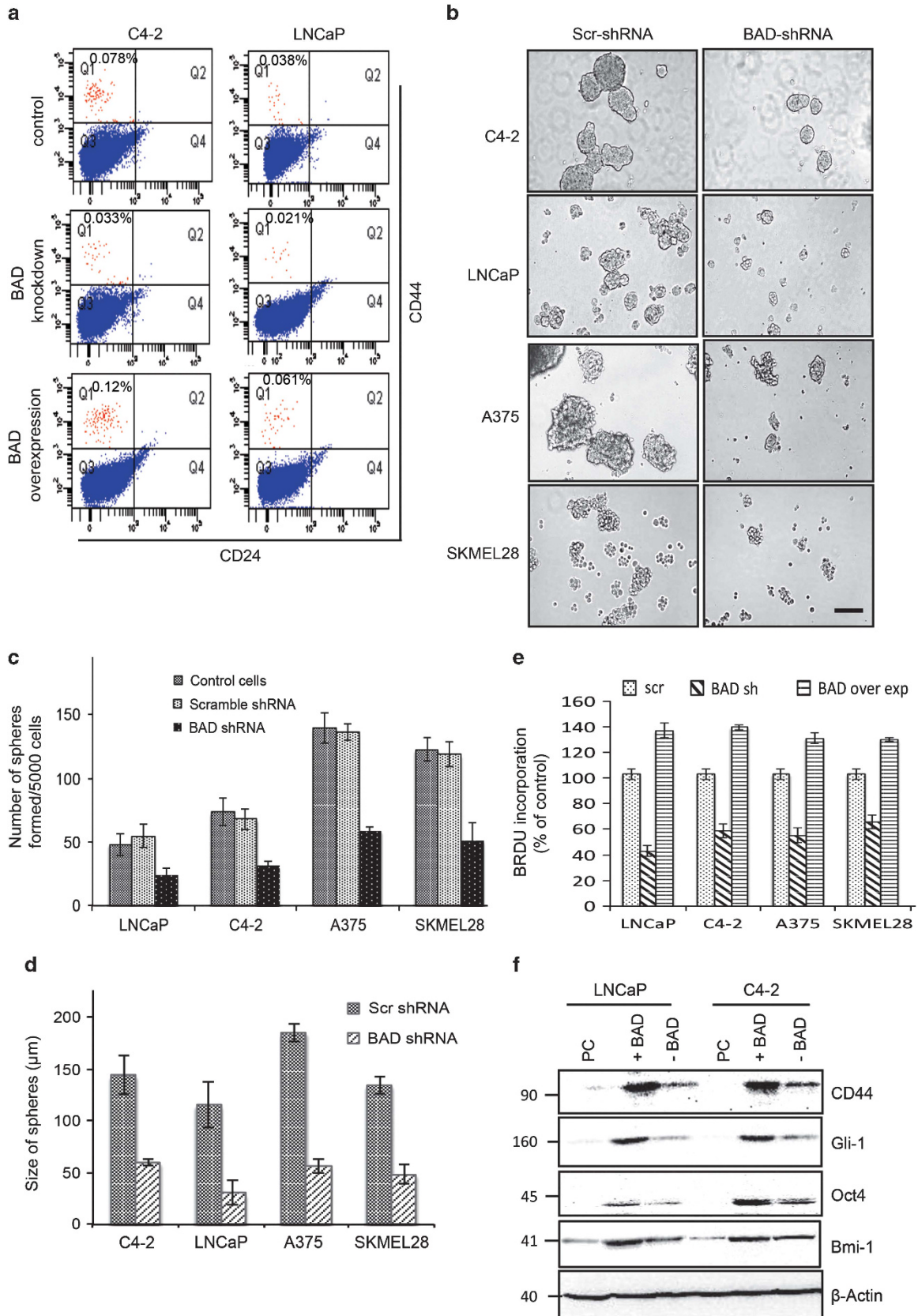
(Gleason Score = 6) suggesting that level of BAD expression might be used as a marker for disease progression. Indeed, BAD expression at the protein and mRNA levels correlated well in various prostate cancer cell lines (Supplementary Figure S6).

Discussion

In this paper, our efforts are focused on understanding the biology of CSCs, with an emphasis on the role of BAD in their survival and self-renewal. As far as we know, this is the first report that comprehensively investigates the importance of BAD in CSC biology as a possible therapeutic target.

The main limitation of using cell lines as source of CSCs is that established cell lines have adapted to *in vitro* culture conditions and may not fully resemble their primary counterparts. However, from a practical perspective, the use of well-characterized established cancer cell lines remain an attractive source of CSC for some mechanistic studies, as primary cells are usually much more difficult to obtain and handle. Because each cancer cell line harbored very minute quantity of CSCs, which are not enough to perform wide variety of experiments presented in this paper, we enriched CSCs by a most widely used tumorosphere formation method and sorted to a purity of 95%. These spheres and CSCs displayed several stem cell-associated properties, including the upregulation of diverse markers for CSC self-renewal and proliferation.

Although the bulk of tumor cells responded to current clinical therapies, the CSCs displayed resistance, resulting in their persistence and enrichment at primary and secondary neoplasms.[47–50] Therefore, it is imperative to identify the mechanisms responsible for the survival and maintenance of CSC in order to design new therapeutic strategies targeting CSCs. Importantly, the non-CSCs display certain degree of plasticity to spontaneously dedifferentiate into CSC phenotype.[51] Therefore, targeting CSCs alone may not yield durable clinical responses, because therapeutic eradication of the existing CSC population might be followed by their regeneration from non-CSCs within the tumor. Thus targeting a 'common' molecule or pathway critical for the survival of both non-CSCs and CSCs is the ultimate therapeutic strategy. Our efforts in this study define the role of BAD in CSC biology and point to BAD as a possible 'common' therapeutic target, because it modulated the survival of both CSCs and non-CSCs.[19] CSCs, in which BAD is both overexpressed and constitutively phosphorylated, were unable to survive in the absence of BAD phosphorylation. *In vivo*, BAD phosphorylation was detected in CSCs of 83% of breast cancer biopsies. Thus results in the present study, and our previous findings in prostate cancer cells that BAD acts as a signaling node where multiple pathways converge, suggest that BAD is a potential target for the elimination of both DCs and CSCs.

Our results show that BAD expression is elevated in a significant number of prostate cancer patient tumors compared with non-malignant tissues. Interestingly, BAD expression positively correlates with the disease stage where high-grade tumors exhibit higher BAD protein levels than those with low-grade cancer, suggesting a role in tumor progression. This is consistent with previous findings, which identified a correlation between BAD immunostaining and increased tumor size in breast cancer patient biopsies.[52] Together, these findings suggest that quantification of BAD levels may be used as a marker for disease progression.

Various pathways are previously described that are essential for the survival of CSCs, although the downstream molecules responsible for survival are not clearly defined.[36–39] We show that the PI3K/Akt and/or Raf/MEK/MAPK pathways are vital for survival and maintenance of CSCs, because inhibition of these key pathways is sufficient to trigger antiproliferative or cell death effects. Interestingly, these survival pathways mediate their effects by controlling BAD phosphorylation in CSCs. We observed a strong correlation between apoptosis and BAD dephosphorylation induced by inhibitors of PI3K, MAPK or Raf in CSCs, suggesting that these drugs alter the BAD phosphorylation to induce cell death. Thus, in addition to modulating the survival of CSCs, BAD is also mediating the cytotoxic effects of drugs or pharmacological inhibitors. It is worth noting that although our data highlight the importance of BAD in CSC survival, the current studies do not rule out the involvement of other essential pathways contributing to CSC survival and drug resistance. In line with this, we noticed an upregulation of BCL-XL protein in CSCs, which may account for the partial effects of BAD dephosphorylation. Combined use of drugs that dephosphorylate BAD and BH3-mimetic induced apoptosis of CSCs more effectively.

In addition to the intrinsic pathways, cancer cells are regulated by extrinsic signals generated in the tumor niche that regulate drug resistance. It is recently shown that CSCs expressed increased growth factor receptors in drug-resistant cancers. For example, prostate and breast CSCs in patient tumors overexpressed EGFR and HER2, respectively.[42,53] It is not clearly known how these aberrant signaling in CSCs imparts resistance to drugs. Our results demonstrate that growth factors rescue CSCs from drug-induced apoptosis by restoring phosphorylation of BAD. Thus, while several therapeutic drugs induce cell death by dephosphorylating BAD, CSCs employ diverse signaling pathways that counter this effect by inducing BAD phosphorylation. In the presence of BAD2SA, which mimics dephosphorylated BAD, none of the survival pathways, such as Akt, MAPK and Raf, nor growth factors like EGF and E2 protected CSCs from apoptosis, emphasizing the potential role of BAD in CSC survival. Thus finding strategies to dephosphorylate BAD may

Figure 5 Depletion of BAD reduces self-renewal of CSCs. (**a**) Control, BAD-depleted and BAD-overexpressed cells were stained with CD44 and CD24 antibodies and analyzed by flow cytometry. (**b**) Cells expressing BAD-shRNA or scrambled-shRNA were used in the sphere formation assay, and the number of spheres formed in 7 days was enumerated. (**c**) Phase-contrast images of spheres expressing BAD-shRNA or scrambled-RNA are shown. Scale bar = 100 μm. (**d**) Sphere size in panel (**b**) was measured using the ImageJ software. (**e**) Control, BAD-depleted and BAD-overexpressed sphere cells were subjected to BrdU proliferation assay as in Figure 1e. (**f**) Upregulation of stemness markers in BAD-overexpressed spheres as compared with parental cells was confirmed by western blotting using the indicated antibodies. The error bars represent S.D. of the biological triplicates. All experiments presented in this figure are representative of four independent experiments
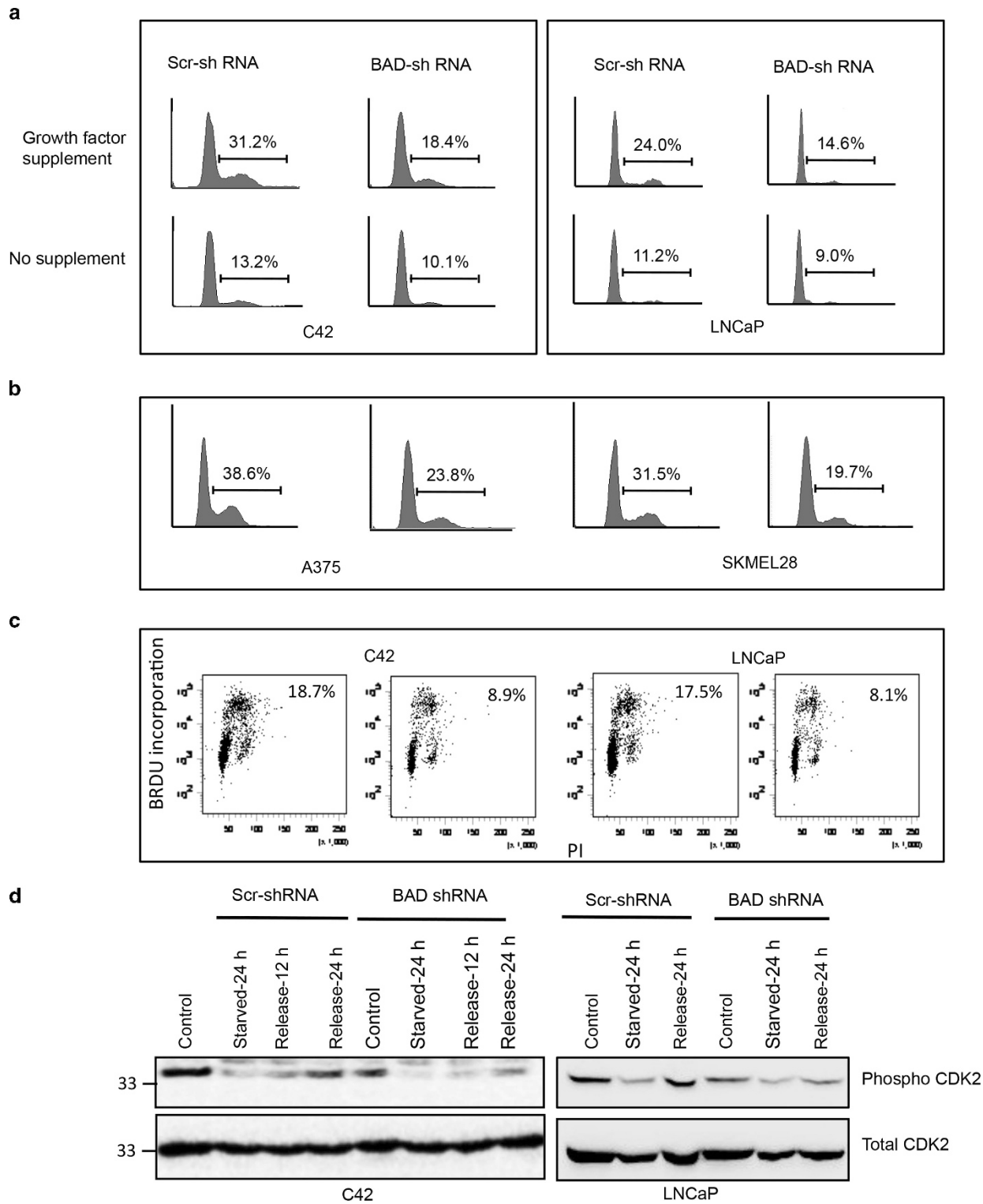
Figure 6 BAD-depleted CSCs are arrested in G0/G1 phase: (**a**) Control and BAD-depleted cells were cultured in sphere-forming conditions for 7 days. Spheres were starved for 1 day where indicated. Single-cell suspension of spheres were stained with propidium iodide and analyzed for DNA content by flow cytometry. (**b**) Cell cycle analysis of melanoma spheres. (**c**) BrdU incorporation and propidium iodide staining of cells in panel (**a**) is shown. The percentage of cells in S phase that are actively synthesizing DNA is shown. (**d**) Control or BAD-depleted cells were cultured in sphere-formation medium for 7 days, and growth was arrested by starving growth factors for 1 day. Then spheres were released from arrest by placing back into medium containing all growth factors, and cell lysates were collected at the indicated time points. Western blotting was performed with phosphoCDK2 and total CDK2 antibodies. All experiments presented in this figure are representative of three independent experiments
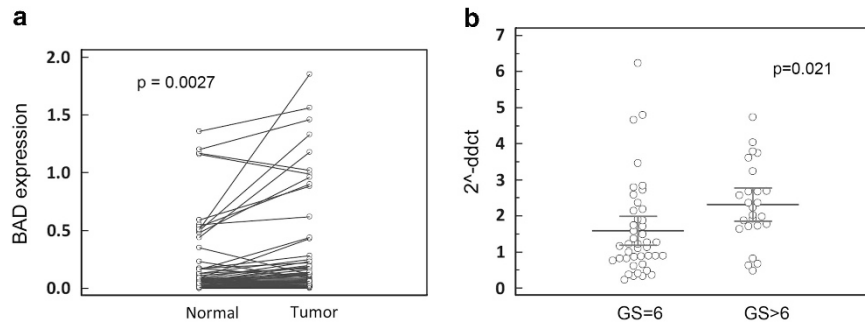
a

b

Figure 7 BAD expression correlates with disease progression. (**a**) BAD expression was measured by quantitative real-time PCR on malignant and non-malignant tumor-adjacent tissue obtained from prostate cancer patients. Tumors expressed more BAD than non-malignant tissue ($P = 0.0027$). (**b**) Tumors were classified into Gleason Score $= 6$ or > 6, and fold-change differences of BAD expression between these two groups were compared. High-grade tumors (GS > 6) expressed more BAD than low-grade (GS < 6) tumors ($P = 0.021$)

be a better therapeutic strategy than targeting each of these pathways individually. Further research is needed to identify kinases or phosphatases that control BAD phosphorylation in CSCs. Identification of BAD kinases and their subsequent inhibition either alone or in combination with BCL-XL inhibitors may provide a better therapeutic strategy for eliminating malignant cancer cells.

Another therapeutic strategy for targeting CSCs involves self-renewal pathways, such as Notch, Hedgehog and Wnt. Nevertheless, targeting these pathways may be limited, because they are also active in normal stem cells and control their self-renewal, proliferation and differentiation. Recently, BCL-2 family proteins such as Mcl-1 are found to be indispensible for self-renewal of stem cells.[54] We have found that depletion of BAD causes a significant decrease in CSC frequency, relative sphere number and size, which is associated with the decrease in S/G2 fraction of the cell cycle. Thus BAD seems to display dual effects on CSCs; while in phosphorylated form it is protecting CSCs from apoptosis, its elevated expression is promoting self-renewal of CSCs and tumor progression. Together, these results suggest that targeting BAD might effectively reduce the CSC number and their self-renewal capacity.

In conclusion, we have demonstrated that BAD phosphorylation is essential for survival of CSCs. Although tested therapeutic drugs exert their toxicities by modulating BAD phosphorylation in CSCs, growth factors counter these effects through the restoration of BAD phosphorylation. Combination of inhibitors that reduce BAD phosphorylation and BCL-XL activity had synergistic proapoptotic effects on CSCs. Moreover, suppression of BAD expression substantially reduced the self-renewal capacity of CSCs. Further studies are needed to validate the role of BAD in CSC survival in an appropriate *in vivo* model.

Materials and Methods

Cell lines and reagents. C4-2 cell line was a gift from Leland Chung (Emory University, Atlanta, GA, USA). All other cell lines were obtained from American Type Culture Collection Center (Manassas, VA, USA). All antibodies unless specified were purchased from Cell Signaling Technology (Beverly, MA, USA). LY294002, PD98059, Z-VAD-FMK, Protein G-agarose beads and DEVD-7-amino-methyl-coumarin (Ac-DEVD-AFC) were from Calbiochem (Chicago, IL, USA). Recombinant human EGF and TNF-α were from Peprotech (Rock Hill, NJ, USA). Vemurafenib was from Selleck Chemicals, Houston, TX, USA. All other chemicals and reagents unless specified were purchased from Sigma (Milwaukee, WI, USA).

Cell culture. All cell lines were maintained in RPMI-1640 medium (Invitrogen, Grand Island, NY, USA) with 10% fetal bovine serum at 37 °C in a humidified incubator of 5% CO_2. In this study, we obtained and enriched CSCs from cell lines of two prostate cancer (androgen-dependent and less aggressive, LNCaP; and androgen-independent and more aggressive, C4-2), two breast cancer (estrogen receptor positive and less metastatic, MCF7; and estrogen receptor negative and more metastatic, MDA-468) and two melanoma (less aggressive, SKMEL28; and more aggressive, A375).

Patient specimen. Formalin-fixed paraffin-embedded archival prostate and breast tumors were obtained from the WCMC-Qatar Genetic Medicine Database and the Arab Breast and Prostate Cancer Consortium Bio-Repository, as described.[55] Prostate specimens were classified into Gleason Score $= 6$ and > 6. ReceoverAll kit (Life Technologies, Grand Island, NY, USA) was used to extract RNA, and BAD expression was quantified by a standard quantitative real-time PCR. Double-immunohistofluorescence analyses of the co-localization of stem cell marker CD44 with phospho-BAD was carried out in 41 breast tumor tissues using a protocol as described.[42] Confocal microscopy was used to obtain fluorescent images.

Sphere culture. Single cells at 1–10 cells/μl were plated on low attachment plates with ultra-low attachment surfaces (Fischer Scientific Co., Pittsburgh, PA, USA) in serum-free DMEM-F12 (1:1) medium supplemented with B27 (Invitrogen), 20 ng/ml EGF, 10 ng/ml basic fibroblast growth factor and 5 μg/ml insulin (hereafter referred to as sphere medium). Growth factors were added to sphere culture every third day. Spheres were collected after 7–10 days and either trypsinized for flow cytometry analysis or protein extracted for western blotting. Where required, sphere number was counted manually using a microscope.

Flow cytometry analysis. Single-cell suspensions of spheres or monolayer cultures were washed in staining solution containing Ca^{2+}- and Mg^{2+}-free PBS with 1 mM EDTA, 25 mM HEPES and 0.5% FBS and incubated with CD44-PE and CD24-APC antibodies (BD Biosciences, San Jose, CA, USA) for 30 min at 4 °C. Cells were rinsed twice in staining solution and either sorted by BD FACSAria II (BD Biosciences) or analyzed by FACS LSRFortessa (BD Biosciences). For cell cycle analysis, cells were pelleted and suspended in 70% ethanol, followed by incubation at 4 °C for 1 h or until further use. Then, cells were pelleted, washed with PBS and incubated for 30 min in 500 μl of buffer containing 50 μg/ml propidium iodide (PI), 20 μg/ml RNase and 0.3% NP40 solution. For BrdU pulse-labeling/PI-staining experiments, cells were pulsed with 20 μM BrdU (Calbiochem) for 3 h, trypsinized and fixed by 70% ethanol. Cells were incubated with 2 M HCl for 20 min and washed with PBS. Cells were incubated with anti-BrdU antibodies and then with anti-mouse-AlexaFlour-647. Finally, cells were incubated in PBS containing 50 μg/ml PI and 20 μg/ml RNAse and analyzed.

Soft agar colony-formation assays. To assess the clonogenicity, 1000 cells in 1.5 ml sphere medium containing 0.35% agarose were overlaid with 1.5 ml 0.5% agarose-containing sphere medium and incubated for 21 days. Images were obtained by a Olympus digital camera (Center Valley, PA, USA), and colonies were counted manually.

Proliferation, migration and invasion assays. BrdU cell proliferation assay kit (Cell Signaling), Colorimetric Cell Migration Assay kit (QCM 24-well, Millipore, Chicago, IL, USA) and Fluorometric Cell Invasion kit (QCM 24-well, Millipore) were used to measure proliferation, migration and invasion capacity of spheres and sorted CSCs, respectively.

Apoptosis and survival assays. Lentiviral production and transduction were performed according to the recommendations of the manufacturer (LentiX system from Clontech, Mountain View, CA, USA). For the analysis of cell survival, day-5 spheres were co-infected with lentiviral vectors containing either BADwt or BAD2SA and luciferase. On day 6, spheres were placed in supplement-free basal DMEM medium and treated with ABT-737. On day 7, spheres were either used for generation of secondary spheres or lysed in cell lysis buffer to measure luciferase activity using a kit from Promega (Madison, WI, USA). To assess the apoptosis, spheres were treated with inhibitors, and growth factors were added 15 min later. After 2–3 days, spheres were lysed in cell lysis buffer and used to assess apoptosis by measuring caspase-3 activity with the Ac-DEVD-AFC as described.[20] Another part of the lysate was used in western blotting. Because of inefficiency of available phospho-BAD antibodies to recognize endogenous BAD, we ectopically expressed HA-BAD and assessed BAD phosphorylation on immunoprecipitated BAD.

RNA interference. Cancer cells were infected with PLL3.7 lentiviral vector containing either shRNA specific to BAD or a scramble-shRNA as reported by us.[20] Three days postinfection, cells were either used in flow cytometry analysis or used in sphere-forming assay to measure the self-renewal capacity of CSCs. Spheres size was measured using the ImageJ software (National Institute of Health, Bethesda, MD, USA).

Statistical analysis. Paired Student's t-test was used to compare differences in BAD expression between normal and tumor tissues. Independent Student's t-test was further applied to compare fold-change differences of BAD expression among samples with $GS = 6$ and samples with $GS > 6$. A P-value < 0.05 was considered significant. All the statistical tests were two sided. Unless otherwise stated, the error bars represent S.D. of the biological triplicates.

Conflict of Interest

The authors declare no conflict of interest.

1. Lapidot T, Sirard C, Vormoor J, Murdoch B, Hoang T, Caceres-Cortes J et al. A cells initiating human acute myeloid leukaemia after transplantation into SCID mice. Nature 1994; **367**: 645–648.
2. Bonnet D, Dick JE. Human acute myeloid leukaemia is organized as a hierarchy that originates from a putative hematopoietic cell. Nat Med 1997; **3**: 730–737.
3. Al-Hajj M, Wicha MS, Benito-Hernandez A, Morrison SJ, Clarke MF. Prospective identification of tumorigenic breast cancer cells. Proc Natl Acad Sci USA 2003; **100**: 3983–3988.
4. Al-Hajj M, Becker MW, Wicha M, Weissman I, Clarke MF. Therapeutic implications of cancer stem cells. Curr Opin Genet Dev 2004; **14**: 43–47.
5. Collins AT, Berry PA, Hyde C, Stower MJ, Maitland NJ. Prospective identification of tumorigenic prostate cancer stem cells. Cancer Res 2005; **65**: 10946–10951.
6. Prince ME, Sivanandan R, Kaczorowski A, Wolf GT, Kaplan MJ, Dalerba P et al. Identification of a subpopulation of cells with cancer stem cell properties in head and neck squamous cell carcinoma. Proc Natl Acad Sci USA 2007; **104**: 973–978.
7. Eramo A, Lotti F, Sette G, Pilozzi E, Biffoni M, Di Virgilio A et al. Identification and expansion of the tumorigenic lung cancer stem cell population. Cell Death Differ 2008; **15**: 504–514.
8. Zhang S, Balch C, Chan MW, Lai HC, Matei D, Schilder JM et al. Identification and characterization of ovarian cancer-initiating cells from primary human tumors. Cancer Res 2008; **68**: 4311–4320.
9. Schatton T, Murphy GF, Frank NY, Yamaura K, Waaga-Gasser AM, Gasser M et al. Identification of cells initiating human melanomas. Nature 2008; **451**: 345–349.
10. Polyak K, Hahn WC. Roots and stems: stem cells in cancer. Nat Med 2006; **2**: 296–300.
11. Dean M, Foio T, Bates S. Tumour stem cells and drug resistance. Nat Rev Cancer 2005; **5**: 275–284.
12. Frank NY, Schatton T, Frank MH. The therapeutic promise of the cancer stem cell concept. J Clin Invest 2010; **120**: 41–50.
13. Konopleva M, Zhao S, Hu W, Jiang S, Snell V, Weidner D et al. The anti-apoptotic genes Bcl-X(L) and Bcl-2 are over-expressed and contribute to chemoresistance of non-proliferating leukaemic CD34 + cells. Br J Haematol 2002; **118**: 521–534.
14. Madjd Z, Mehrjerdi AZ, Sharifi AM, Molanaei S, Shahzadi SZ, Asadi-Lari M. CD44 + cancer cells express higher levels of the anti-apoptotic protein Bcl-2 in breast tumours. Cancer Immun 2009; **9**: 4.
15. Datta SR, Dudek H, Tao X, Masters S, Fu H, Gotoh Y et al. Akt phosphorylation of BAD couples survival signals to the cell-intrinsic death machinery. Cell 1997; **91**: 231–241.
16. Harada H, Becknell B, Wilm M, Mann M, Huang LJ, Taylor SS et al. Phosphorylation and inactivation of BAD by mitochondria-anchored protein kinase A. Mol Cell 1999; **3**: 413–422.
17. Shimamura A, Ballif BA, Richards SA, Blenis J. Rsk1 mediates a MEK-MAP kinase cell survival signal. Curr Biol 2000; **10**: 127–135.
18. Schürmann A, Mooney AF, Sanders LC, Sells MA, Wang HG, Reed JC et al. p21-activated kinase 1 phosphorylates the death agonist bad and protects cells from apoptosis. Mol Cell Biol 2000; **20**: 453–461.
19. Sastry KS, Smith AJ, Karpova Y, Datta SR, Kulik G. Diverse anti-apoptotic signaling pathways activated by Vasoactive Intestinal Peptide, Epidermal Growth Factor and PI3 Kinase in prostate cancer cells converge on BAD. J Biol Chem 2006; **281**: 20891–20901.
20. Sastry KS, Karpova Y, George K. Epidermal growth factor protects prostate cancer cells from apoptosis by inducing BAD phosphorylation via redundant signaling pathways. J Biol Chem 2006; **281**: 27367–27377.
21. Sastry KS, Karpova Y, Prokopovich S, Smith AJ, Essau B, Gersappe A et al. Epinephrine protects cancer cells from apoptosis via activation of Protein Kinase A and BAD phosphorylation. J Biol Chem 2007; **282**: 14094–14100.
22. Smith AJ, Karpova Y, D'Agostino R Jr, Willingham M, Kulik G. Expression of the Bcl-2 protein BAD promotes prostate cancer growth. PLoS One 2009; **4**: e6224.
23. Cannings E, Kirkegaard T, Tovey SM, Dunne B, Cooke TG, Bartlett JM. Bad expression predicts outcome in patients treated with tamoxifen. Breast Cancer Res Treat 2007; **102**: 173–179.
24. Craik AC, Veldhoen RA, Czernick M, Buckland TW, Kyselytzia K, Ghosh S et al. The BH3-only protein Bad confers breast cancer taxane sensitivity through a nonapoptotic mechanism. Oncogene 2010; **29**: 5381–5391.
25. Marchion DC, Cottrill HM, Xiong Y, Chen N, Bicaku E, Fulp WJ et al. BAD phosphorylation determines ovarian cancer chemosensitivity and patient survival. Clin Cancer Res 2011; **17**: 6356–6366.
26. Sheridan C, Brumatti G, Martin SJ. Oncogenic B-Raf^{V600E} inhibits apoptosis and promotes ERK-dependent inactivation of Bad and Bim. J Biol Chem 2008; **238**: 22128–22135.
27. La Porta CA, Zapperi S. Human breast and melanoma cancer stem cells biomarkers. Cancer Lett 2013; **338**: 69–73.
28. Zapperi S, La Porta CA. Do cancer cells undergo phenotypic switching? The case for imperfect cancer stem cell markers. Sci Rep 2012; **2**: 441.
29. Ponti D, Costa A, Zaffaroni N, Pratesi G, Petrangolini G, Coradini D et al. Isolation and in vitro propagation of tumorigenic breast cancer cells with stem/progenitor cell properties. Cancer Res 2005; **65**: 5506–5511.
30. Yan W, Chen Y, Yao Y, Zhang H, Wang T. Increased invasion and tumorigenicity capacity of CD44 +/CD24- breast cancer MCF7 cells in vitro and in nude mice. Cancer Cell Int 2013; **13**: 62.
31. Fillmore C, Kuperwasser C. Human breast cancer cell lines contain stem-like cells that self-renew, give rise to phenotypically diverse progeny and survive chemotherapy. Breast Cancer Res 2008; **10**: R25.
32. Yin H, Glass J. The phenotypic radiation resistance of CD44 +/CD24 − or low breast cancer cells is mediated through the enhanced activation of ATM signaling. PLoS One 2011; **6**: e24080.
33. Hurt EM, Kawasaki BT, Klarmann GJ, Thomas SB, Farrar WL. CD44 + CD24(−) prostate cells are early cancer progenitor/stem cells that provide a model for patients with poor prognosis. Br J Cancer 2008; **98**: 756–765.
34. Tan Y, Demeter MR, Ruan H, Comb MJ. BAD ser-155 phosphorylation regulates BAD/Bcl XL interaction and cell survival. J Biol Chem 2000; **18**: 25865–25869.
35. Oltersdorf T, Elmore SW, Shoemaker AR, Armstrong RC, Augeri DJ, Belli BA et al. An inhibitor of Bcl-2 family proteins induces regression of solid tumours. Nature 2005; **435**: 677–681.
36. Majumdar PK, Sellers WR. Akt-regulated pathways in prostate cancer. Oncogene 2005; **14**: 7465–7474.
37. Faivre S, Djelloul S, Raymond E. New paradigms in anticancer therapy: targeting multiple signaling pathways with kinase inhibitors. Semin Oncol 2006; **33**: 407–420.
38. Gollob JA, Wilhelm S, Carter C, Kelley SL. Role of Raf kinase in cancer: therapeutic potential of targeting the Raf/MEK/ERK signal transduction pathway. Semin Oncol 2006; **33**: 392–406.
39. Mimeault M, Batra SK. New promising drug targets in cancer- and metastasis-initiating cells. Drug Discov Today 2010; **15**: 354–364.
40. Clark GM, McGuire WL. Steroid receptors and other prognostic factors in primary breast cancer. Semin Oncol 1988; **15**: 20–25.

41. Allred DC, Brown P, Medina D. The origins of estrogen receptor α-positive and estrogen receptor α-negative human breast cancer. *Breast Cancer Res* 2004; **6**: 240–245.

42. Mimeault M, Johansson SL, Batra SK. Pathobiological implications of the expression of EGFR, pAkt, NF-κB and MIC-1 in prostate cancer stem cells and their progenies. *PLoS One* 2012; **7**: 31919.

43. Mazzoleni S, Politi LS, Pala M, Cominelli M, Franzin A, Sergi Sergi L *et al.* Epidermal growth factor receptor expression identifies functionally and molecularly distinct tumor-initiating cells in human glioblastoma multiforme and is required for gliomagenesis. *Cancer Res* 2010; **70**: 7500–7513.

44. Diaz A, Leon K. Therapeutic approaches to target cancer stem cells. *Cancers* 2011; **3**: 3331–3352.

45. Zinkel S, Gross A, Yang E. BCL2 family in DNA damage and cell cycle control. *Cell Death Differ* 2006; **13**: 1351–1359.

46. Jablonska B, Aguirre A, Vandenbosch R, Belachew S, Berthet C, Kaldis P *et al.* Cdk2 is critical for proliferation and self-renewal of neural progenitor cells in the adult subventricular zone. *J Cell Biol* 2007; **179**: 1231–1245.

47. Gupta PB, Onder TT, Jiang G, Tao K, Kuperwasser C, Weinberg RA *et al.* Identification of selective inhibitors of cancer stem cells by high-throughput screening. *Cell* 2009; **138**: 645–659.

48. Mimeault M, Hauke R, Batra SK. Recent advances on the molecular mechanisms involved in the drug resistance of cancer cells and novel targeting therapies. *Clin Pharmacol Ther* 2008; **83**: 673–691.

49. Li X, Lewis MT, Huang J, Gutierrez C, Osborne CK, Wu MF *et al.* Intrinsic resistance of tumorigenic breast cancer cells to chemotherapy. *J Natl Cancer Inst* 2008; **100**: 672–679.

50. Bao S, Wu Q, McLendon RE, Hao Y, Shi Q, Hjelmeland AB *et al.* Glioma stem cells promote radioresistance by preferential activation of the DNA damage response. *Nature* 2006; **444**: 756–760.

51. Chaffer CL, Brueckmann I, Scheel C, Kaestli A, Wiggins PA, Rodrigues LO *et al.* Normal and neoplastic nonstem cells can spontaneously convert to a stem-like state. *Proc Natl Acad Sci USA* 2011; **108**: 7950–7955.

52. Al-Bazz YO, Underwood JC, Brown BL, Dobson PR. Prognostic significance of Akt, phospho-Akt and BAD expression in primary breast cancer. *Eur J Cancer* 2009; **45**: 694–704.

53. Korkaya H, Wicha MS. HER2 and breast cancer stem cells: More than meets the eye. *Cancer Res* 2013; **73**: 3489–3493.

54. Singh S, Bora-Singhal N, Kroeger J, Laklai H, Chellappan SP. βArrestin-1 and Mcl-1 modulate self-renewal growth of cancer stem-like side-population cells in non-small cell lung cancer. *PLoS One* 2013; **8**: 55982.

55. Shan J, DSouza SP, Bakhru S, Al-Azwani EK, Ascierto ML, Sastry KS *et al.* TNRC9 downregulates BRCA1 expression and promotes breast cancer aggressiveness. *Cancer Res* 2013; **73**: 2840–2849.